European Journal of Orthopaedic Surgery & Traumatology (2019) 29:47–50
https://doi.org/10.1007/s00590-018-2287-7

ORIGINAL ARTICLE • WRIST - BIOMECHANICS

Maximum loading of carpal bones during movements: a finite element study

H. Oflaz[1] · I. Gunal[2]

Received: 24 May 2018 / Accepted: 1 August 2018 / Published online: 3 August 2018

Abstract

Background Maximum stresses show critical points on an object because failure may start from the area close to maximum stress points. However, there appears no study on maximum loading points of carpal bones.

Purpose To clarify the loading pattern of each carpal bone during wrist movements.

Methods A finite element wrist model was designed using a three-dimensional reconstruction of computed tomographic images from the distal end of radius and ulna to the proximal third of metacarpals. Loading was performed in neutral, 45° of flexion and extension, 5° of radial and 25° of ulnar deviation, and maximum loading points were plotted.

Results In each position except for extension, minimum loads were carried by triquetrum, while minimum loads were carried by capitatum in extension. Maximum loads were carried by trapezium in neutral and ulnar deviation and flexion but by scaphoideum in radial deviation and extension.

Conclusion Studies on maximum loading of each bone are a new approach and may help to improve the knowledge on wrist mechanics.

Keywords Finite element modeling · Wrist biomechanics · Maximum loading

Introduction

The biomechanics of the wrist is complex, and load transmission through the radiocarpal joint is essential in order to understand the issue. Although several studies had been conducted for this purpose [2, 5, 6, 13], review of the literature revealed no study on the maximal loads in each carpal bone during movement. However, maximum stresses show critical points on an object because failure may start from the area close to maximum stress points [9]. In the present study, we evaluated maximum loading of the carpal bones during wrist movements in a three-dimensional model by applying finite element method (FEM).

FEM is a numerical method to solve boundary value matters for partial differential equations by offering approximate solutions. It divides large equations into smaller equations to simplify it, and those simpler parts are called finite elements. Assembly of those finite elements and their simple equations form the entire problem. FEM as an essential complement for the in vitro biomechanical evaluations has been widely used on bone models [8, 16]. In this study, the FEM is used on structural wrist model to predict stresses on each fragment of the entire model.

In the present study, we tried to answer whether some disorders or fracture mechanisms of carpal bones are explained by maximum loading points approach using FEM.

Materials and methods

A wrist model was designed using a three-dimensional reconstruction of computed tomographic images from the distal end of radius and ulna to the proximal third of metacarpals of a 25-year-old man who gave informed consent. The patient had no history of hand trauma or illness before. Images were considered as normal by a senior radiologist.

I. Gunal–Retired. Formerly Professor at Department of Orthopedics, Dokuz Eylul University Hospital.

✉ I. Gunal
izge.gunal@gmail.com

[1] HGO Ind. and Trade Inc., Izmir, Turkey

[2] Department of Orthopedics, Dokuz Eylul University Hospital, Maltepe Mah. 124 Sokak, No: 4, 35310 Guzelbahce, Izmir, Turkey

Images of neutral position were taken with the wrist in neutral forearm rotation, 20° of extension and neutral radial/ulnar deviation. Then, the DICOM images were transferred to Mimics 17.0 (Materialise Corp, Leuven, Belgium) to form 3D models of the wrist. Then, the 3D models of the wrist were transferred into solid part to be able to make a finite element analysis. FEM was applied in ANSYS 16.1 (ANSYS, Inc., Canonsburg, PA, USA) on constructed wrist models. The radius and ulna were fixed from their distal tip, so that they were handled as immobile rigid bodies [2].

The radius and ulna were designed as having elastic modulus of 10 GPa and the Poisson ratio 0.22 like cortical bone [3]. Bones on the wrist model were designed as having elastic modulus of 0.5 GPa and the Poisson ratio 0.3 like cancellous bone [11]. The pisiform was not included in the analysis. Cartilage elements were incorporated external borders of bones and assumed to have elastic modulus 7 MPa a Poisson ratio 0.3 [1, 2, 15]. Ligaments were placed as nonlinear spring models, and rigidities and origin and insertion were estimated from the previously published study of Horii et al. [7] (Fig. 1). The stiffness constant for the springs was also determined from previous series [2, 7].

Loading was performed in neutral, 45° of flexion and extension, 5° of radial and 25° of ulnar deviation. To the distal end of the metacarpals, 255.6, 120.3, 106.4, 88.0 and 77.3 N forces were applied, respectively, from first to fifth [2, 5]. The direction of loading was along the long axis of metacarpals [2, 5]. First, the loads acting on radius and ulna were measured and compared with those previously published series [2, 5, 13] in order to validate the system used in the study. Then, maximum loading in the bones was measured in neutral, flexion, extension, radial and ulnar deviation.

Results

In the first part of the study, 79% of the loads were carried by radius and 21% by ulna. Load distribution in radiocarpal joint was 62% in scaphoradial, 17% in lunoradial and 21% in lunoulnar direction. This distribution was as 27% in scaphotrapeziotrapezoidal, 29% in lunocapitate and 44% in triquetrolunohamate interface through midcarpal joint. These results were comparable with the previous studies performed by 3D analysis [5], 2D analysis [2] or cadaveric [7] studies.

Then, maximum loads carried by each carpal bone in neutral, flexion, extension, radial and ulnar deviation are displayed in Table 1. In each position except for extension, minimum loads were carried by triquetrum, while minimum loads were carried by capitatum in extension (Table 1). Maximum loads were carried by trapezium in neutral and ulnar deviation and flexion but by scaphoideum in radial deviation and extension (Table 1).

The position of maximum loads during radioulnar deviation is illustrated in Fig. 2. In trapezium, maximum

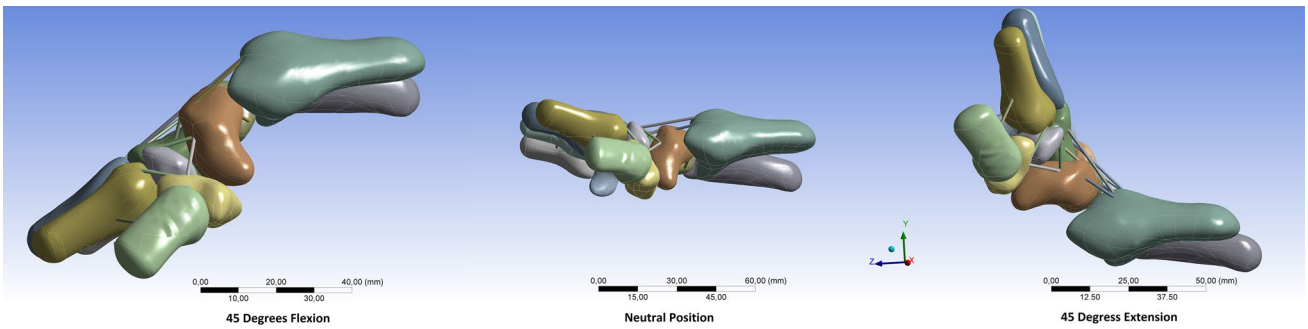

Fig. 1 Construction of the system

Table 1 Maximum loading (MPa) of the carpal bones

	Neutral position	5° Radial deviation	25° Ulnar deviation	45° Flexion	45° Extension
Trapezium	138.41	59.443	93.905	161.13	111.34
Trapezoideum	49.689	25.257	40.706	91.337	39.216
Capitatum	45.015	24.755	31.209	49.855	37.124
Hamatum	92.99	24.457	26.539	66.774	54.318
Triquetrum	34.813	7.3232	14.057	26.816	39.399
Scaphoideum	111.4	61.098	50.455	109.84	112.38
Lunatum	22.094	26.211	22.815	78.246	24.656

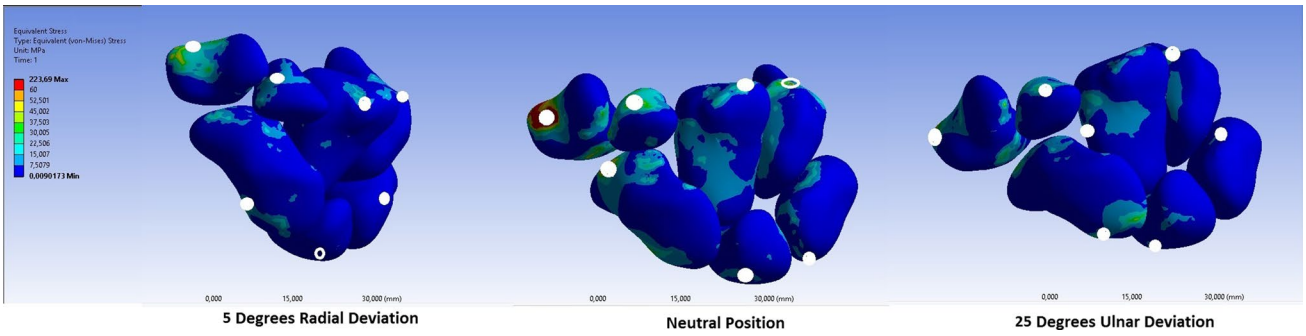

Fig. 2 Maximum loading points of each carpal bone during radioulnar deviation

loading was always in the palmar portion of distal articular surface, but slightly moving to ulnar direction, while the wrist is moving from radial to ulnar. Maximum loading was always in the middle of distal articular in trapezoideum with almost no change. This was also similar of maximal loading of hamatum. Capitatum showed maximum loading in the distal articular surface in neutral and radial deviation, but moved to capitohamate joint in ulnar deviation. Lunatum showed constant maximum loading in radiolunate joint. Scaphoideum and triquetrum displayed reciprocal loading during movements that while maximum loading of scaphoideum was in proximal part in radial and ulnar deviations but in distal in neutral position, triquetrum loaded maximally in distal part in radial and ulnar deviations but in proximal in neutral position (Fig. 2).

The points of maximum loading were constant during flexion–extension movement (Fig. 3). Maximum loads were observed in the proximal parts of lunatum and triquetrum both in flexion and extension, but in the distal parts of the remaining carpal bones (Fig. 3).

Discussion

In the present study, we performed a three-dimensional finite element analysis of the carpal bones from 5° of radial deviation to 25° of ulnar deviation and from 45° of flexion to 45° of extension with special regard to the maximum loads carried by each carpal bone. Such an approach is mandatory for maximum stresses which show critical points on an object because failure may start from the area close to maximum stress points [9], and this may be useful in order to explain common wrist problems such as fractures, osteoarthritis or avascular necrosis.

The validity of the model was confirmed by comparing our results with the previous studies. In the present study, 79.0% of the loads were transmitted to radius and 21.0% to ulna. This ratio was 86.3 and 13.7 in the three-dimensional FEM by Gislason et al. [5], 81.0 and 19.0 in the two-dimensional FEM by Bicen et al. [2], and 81.6 and 18.4 in the cadaveric study of Palmer and Warner [13].

Sure, the present study has several limitations. First, the model used in the study is a wrist of a healthy individual. This may be overcome by more studies. Second, loading of the wrist in different degrees of circumduction movement is mandatory for more understanding of the wrist mechanics,

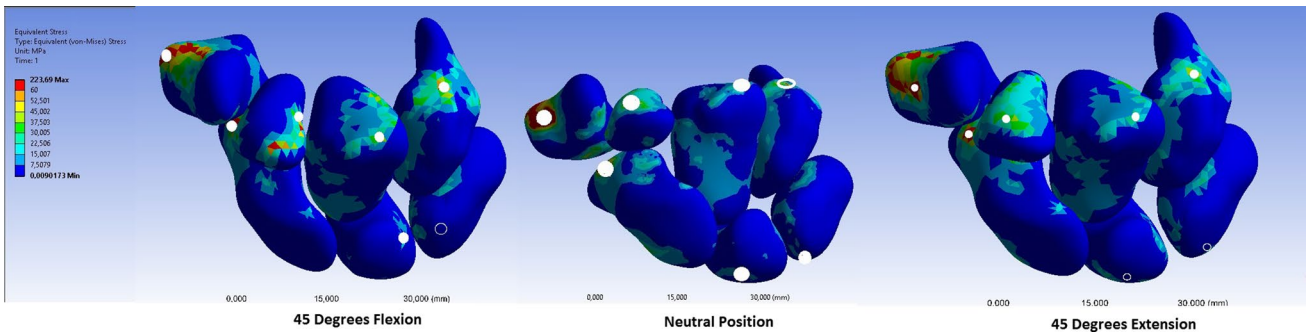

Fig. 3 Maximum loading points of each carpal bone during flexion and extension

but the results of this study may a beginning for such a purpose.

In almost all positions, maximum loading points were in trapezium followed by scaphoideum (Table 1). This finding may explain the relatively high prevalence of osteoarthritis in the first carpometacarpal (CMC), radioscaphoid and scaphotrapeziotrapezoidal joints [14]. Similarly, the reason of low risk of osteoarthritis [10] around the triquetral bone may be relatively low peak loads carried by this bone (Table 1).

It is well known that first CMC arthrosis begins from the palmar and radial surface of the joint [12]. The findings of the present study are in accordance with the literature that maximum loads are carried in the palmar and radial aspect of distal articular surface of trapezium (Fig. 2). Similar findings were also recognized for lunatum that maximum loading was always in the center of the radiolunate joint (Fig. 2). The difference is in the position of the wrist where the maximum loads decrease, that is, radial deviation for trapezium but not for lunatum (Table 1). From these results, we can suggest to immobilize the wrist in radial deviation to unload trapezium and avoid from radial deviation for the cases to unload lunatum.

Maximum loads were always measured in the middle of distal articular surface of trapezoideum (Fig. 2). For some of the loads are carried by trapezoideum, maybe some operations using this part as a graft [4] should be handled with caution.

While maximum loading of hamatum was always in distal articular surface, capitatum showed maximum loading in the distal articular surface in neutral and radial deviation, but moved to capitohamate joint in ulnar deviation. We do not know how to comment on this finding but should be kept in mind in explaining carpal mechanics.

An interesting finding of the present study is the reciprocal loading scaphoideum and triquetrum during movements that while maximum loading of scaphoideum was in proximal part in radial and ulnar deviations but in distal in neutral position, triquetrum loaded maximally in distal part in radial and ulnar deviations but in proximal in neutral position (Fig. 2). Scaphoideum has very complex movements during wrist motion, especially to connect proximal row to distal row. Triquetrum seems to balance scaphoid throughout the range of motion.

The points of maximum loading were constant during flexion–extension movement (Fig. 3). Maximum loads were observed in the proximal parts of lunatum and triquetrum both in flexion and extension, but in the distal parts of the remaining carpal bones (Fig. 3).

In order to minimize the maximum loads, we may say to immobilize the wrist in radial deviation and extension for disorders of trapezium, trapezoideum, capitatum and hamatum; in radial deviation and flexion for triquetrum; ulnar deviation and flexion for scaphoideum; and neutral position for lunatum (Table 1).

Improved recognition of carpal bone loading may help for better understanding of some disorders and consequently the management.

Compliance with ethical standards

Conflict of interest The authors declare that they have no competing interests.

References

1. Beardsley CL, Heiner AD, Marsh JL et al (1999) Mechanical characterization of a bone fracture surrogate. Presented at the 23rd annual meeting of the American Society of Biomechanics. University of Pittsburgh, 21–23 Oct 1999
2. Bicen AC, Gokdemir H, Seber S et al (2015) Load transmission characteristics of limited carpal fusions: a two-dimensional finite element study. Eur J Orthop Surg Traumatol 25(2):305–308
3. Chamoret D, Roth S, Feng Z-Q et al (2013) A novel approach to modelling and simulating the contact behaviour between a human hand model and a deformable object. Comput Methods Biomech Biomed Eng 16(2):130–140
4. Cuenod P (1999) Osteoligamentoplasty and limited dorsal capsulodesis for chronic scapholunate dissociation. Ann Chir Memb Super 18(1):38–53
5. Gíslason MK, Stansfield B, Bransby-Zachary M et al (2012) Load transfer through the radiocarpal joint and the effects of partial wrist arthrodesis on carpal bone behavior: a finite element study. J Hand Surg 37E(9):871–878
6. Gunal I, Ozcan O, Uyulgan B et al (2005) Biomechanical analysis of load transmission characteristics of limited carpal fusions used to treat Kienböck's disease. Acta Orthop Traumatol Turc 39(4):351–355
7. Horii E, Garcia-Elias M, Bishop AT et al (1990) Effect on force transmission across the carpus in procedures used to treat Kinböck's disease. J Hand Surg 15A(3):393–400
8. Kim HJ, Chun HJ, Moon SH et al (2010) Analysis of biomechanical changes after removal of instrumentation in lumbar arthrodesis by finite element analysis. Med Biol Eng Comput 48(7):703–709
9. Ko C, Brown TD (2007) A fluid-immersed multi-body contact finite element formulation for median nerve stress in the çarpal tunnel. Comput Methods Biomech Biomed Eng 10(5):343–349
10. Kofman KE, Schuurman AH, Mulder MC et al (2014) The pisotriquetral joint: osteoarthritis and enthesopathy. J Hand Microsurg 6(1):18–25
11. Kubicek M, Florian Z (2009) Stress strain analysis of knee joint. Eng Mech 16(3):315–322
12. Moulton MJ, Parentis MA, Kelly MJ et al (2001) Influence of metacarpophalangeal joint position on basal joint-loading in the thumb. J Bone Jt Surg 83A(5):709–716
13. Palmer AK, Werner FW (1984) Biomechanics of the distal radioulnar joint. Clin Orthop 187:26–35
14. Scordino LE, Bernstein J, Nakashian M et al (2014) Radiographic prevalence of scaphotrapeziotrapezoid osteoarthrosis. J Hand Surg 39A(9):1677–1682
15. Silver FH, Bradica G, Tria A (2002) Elastic energy storage in human articular cartilage: estimation of the elastic modulus for type II collagen and changes associated with osteoarthritis. Matrix Biol 21(2):129–137
16. Xiao Z, Wang L, Gong H, Zhu D (2012) Biomechanical evaluation of three surgical scenarios of posterior lumbar interbody fusion by finite element analysis. Biomed Eng Online 11:31